Decentralised Hydrogen Fuelled Gas Engine CHP Units: A Feasibility Study with Modelica

Florian Andreas Beerlage[1] Naqib Salim[1] Maurice Kettner[1]

[1]Institute of Refrigeration, Air-Conditioning and Environmental Engineering, Karlsruhe University of Applied Sciences, Germany, florian.beerlage, muhamad_naqib.md_salim, maurice.kettner@h-ka.de

Abstract

The use of hydrogen gas as an alternative fuel to power energy systems has been a topic of research over the last few decades and is currently gaining importance, even more due to current circumstances related to decarbonise energy supply. One focus of research is the use of hydrogen gas in combined heat and power gas engines, as this type of energy conversion is known for its high efficiency. For this reason, a cross-border project between France and Germany is developing a living laboratory in the Upper Rhine region to investigate the feasibility of hydrogen gas as an alternative fuel in a holistic decentralised energy system[1]. It consists of several energy components, including a polymer electrolyte membrane electrolyser (PEMEC), gas engine combined heat and power (CHP) unit, photovoltaic (PV) panels, hydrogen storage, thermal and electrical energy storage. To enable and demonstrate multiple what-if scenarios of possible variations of the energy system, a simulation model was developed using Modelica. Users, e.g. local authorities, landlords, businessman etc., of this simulation model could utilize it as a decision support tool for designing a carbon neutral energy system for their own use. This paper describes the development of the model and its application with real measured data from municipal buildings in the city of Offenburg, Germany. The results indicate that the suitability of the model and the use of hydrogen CHPs can be beneficial for this specific use case.

Keywords: Hydrogen, HVAC, CHP, Electrolyser, Gas engine, Cogeneration

1 Introduction

The primary motivation for undertaking these projects is the ambitious objective to reduce greenhouse gas emissions. Germany set goals to reduce these by at least 65% by 2030 and 88% by 2040, compared to 1990 levels (Umweltbundesamt 2023b). These goals align with the Paris Agreement and the Kyoto Protocol, forming part of the climate protection strategies of the EU and the United Nations. Given these targets, hydrogen is likely to play a crucial role in the energy transition due to its potential for carbon-neutral production. On 14^{th} November 2023, Germany's Vice-Chancellor Robert Habeck announced a plan for a 9,700 km hydrogen network, set to start in 2024. This network is part of the European Hydrogen Backbone initiative, comprised of thirty-three energy infrastructure operators with a vision for a climate-neutral Europe supported by a renewable and low-carbon hydrogen market (Reuters 2023; European Hydrogen Backbone 2024). Despite the initiative's early stage, concerns have been raised about the inclusion of small and medium-sized locations, with Offenburg, for example, not being connected to the hydrogen backbone until 2035. Yet, Offenburg aims for carbon neutrality, partly through hydrogen as a green energy carrier. Given that the city already operates gas engine CHP units, an investigation into the feasibility of transitioning them to hydrogen is required. When comparing hydrogen-based gas engine CHP units with fuel cell CHP units, both offer the advantage of no green house gas emissions. While fuel cells have higher electrical efficiency, gas engines often provide better thermal efficiency due to higher combustion temperatures. Additionally, gas engines benefit from shorter startup times and the capability for modulation (Ellamla et al. 2015; Elmer et al. 2015). The purchase, installation and operating costs of gas engine CHP units are also generally lower (see (Danish Energy Agency 2024)). To ensure a precise and practical investigation, measurement data concerning heat and electricity demand from five communal buildings were provided, which are located in Offenburg[2].

This paper is structured as follows: Section 2 describes the model considered in this study and the equations implemented in the newly developed modules. Section 3 presents the validation of the model. Section 4 details the construction, simulation and results of a case study using the data provided by the city of Offenburg. Lastly, section 5 discusses the results and outlines future work.

2 Schematic Model Description

Wherever possible, open-source Modelica libraries compatible with OpenModelica were integrated to ensure the software remains open-source. The *Modelica Buildings library* was utilized for modeling PV systems, batteries, and the grid (Wetter et al. 2014). For the heat pump, an

[1]For more information please visit this website: https://co2inno.com

[2]The software is compatible with OpenModelica and will be published here: https://github.com/IKKUengine

 10.3384/ECP207 80 DOI

empirical approach was adopted based on Ruhnau et al. (2019) for both accuracy and to simplify programming. This methodology allows for the selection between air-, ground-, and water-source heat pumps, as well as between floor heating or radiator heating. Additionally, a simplified thermal energy storage system was implemented to facilitate easier control of the CHP units. This section outlines the modeling methodology for gas engine CHP units, PEMEC, hydrogen storage, compressors, and control strategies.

Table 1. Notation

A_{mem}	m^2	Area membrane
CF		Correction factor
E	V	Operating voltage
E_0	V	Reversible cell voltage
$E_{act,k}$	kJ/mol	Activation energy
F	C/mol	e Faraday constant
I_{cell}	A	Cell current
$J_{0,k}$	A/m^2	Current exchange density at k
J_{cell}	A/m^2	Current exchange density at the anode or cathode
J_0^{ref}	A/m^2	Reference exchange current density
LHV_i	kWh/kg	Lower heating value
M_i	kg/mol	Molar mass of i
P	W	Electrical power
R	$J/(mol \cdot K)$	Universal gas constant
R_{ohm}	Ω	Resistance
SOC		State of Charge of the storage
T	K	Temperature in Kelvin
$\dot{Q}_i$	W	Heat flow
$\dot{V}_i$	Nm^3/h	Volume flow
V_{act}	V	Activation voltage
V_{cell}	V	Cell voltage
V_{con}	V	Transport voltage
V_{ohm}	V	Ohmic voltage
V_{oc}	V	Open circuit voltage
V_{tn}	V	Thermo-neutral voltage
Y		Minimum threshold
Z		Modulation of the CHP plant
m_i	kg	Total mass of fuel needed
$\dot{m}_i$	kg/s	Mass flow rate
n_i		Count
p_i	Pa	Pressure
v_i		Stoichiometric coefficients
α_k		Symmetry factor
σ_{mem}	S/m	Proton conductivity of the membrane
ν		Relative difference
ΔG	kJ/mol	Gibbs free energy
ΔH	kJ/mol	Work enthalpy

2.1 Gas Engine CHP

Two different modelling approaches were carried out. The first one being a gas engine CHP operating with a stationary heat and power output under nominal conditions. Second, an empirical approach was used for a gas engine CHP model that can follow a heat load up to a given maximum and minimum modulation. Both models are designed for heat-driven operation, where sizing and operation are based on the heat demand of the consumer. This is because heat-guided CHPs are the most common (Arbeitsgruppe Erneuerbare Energien-Statistik 2015, pp. 16–17).

One of the most important key performance indices for an gas eninge CHP are the utilisation hours τ. These will help to evaluate the performance of the CHP later on and is defined as:

$$\tau = \frac{E_{CHP,a}}{P_{nom}} \tag{1}$$

where $E_{CHP,a}$ is the energy delivered within one year and P_{nom} is the nominal power of the cogeneration unit. This value can be calculated using either thermal or electrical energy. In this paper only heat energy and power will be considered due to the fact that the CHP is heat guided.

2.1.1 Stationary Gas Engine CHP Model

Normally, gas engine CHP units are running under nominal conditions. Excess heat is stored in a buffer tank. Electricity is either consumed, stored in the battery (BAT) or fed into the grid. When the load is lower, the efficiency of the CHP decreases, so a minimum threshold Y is set as a turn-on condition, which by default is ≥ 50 %:

$$Y = \frac{P_{th,dem}}{P_{th,nom}}, \tag{2}$$

where $P_{th,dem}$ is the thermal heat demand and $P_{th,nom}$ is the thermal heat production of the CHP at nominal conditions. In order to determine the fuel consumption, nominal efficiencies are required. Thereby η_{el} is the ratio of the electrical power P_{el} and the fuel power P_f:

$$\eta_{el} = \frac{P_{el}}{P_f}, \tag{3}$$

and η_{th} – also called heat yield – is the ratio of the useful heat output (thermal power) P_{th} and the fuel power:

$$\eta_{th} = \frac{P_{th}}{P_f}. \tag{4}$$

Since the gas engine is able to be fueled with natural gas, hydrogen, or gas- hydrogen mixture, the fuel power is calculated by:

$$P_f = \sum \dot{m}_i \cdot LHV_i, \tag{5}$$

where $\dot{m}_i$ represents the fuel mass flow rate of i representing CH_4 or H_2 and LHV_i is the lower heating value of

the fuel (compare table 2). The total mass of fuel required can be determined as follows:

$$m_i = \int \dot{m}_i \, dt \tag{6}$$

Table 2. LHV of different fuels (Bender et al. 2020, p. 805)

	value	unit
LHV_{H_2}	33.3	kWh/kg
LHV_{CH_4}	13.9	kWh/kg

2.1.2 Modulation Gas Engine CHP Model

The modulation CHP model is based on an empirical modelling approach based on Berberich et al. (2015) and Höfner (2019). The electrical efficiency is exclusively a function of the nominal electrical power of the CHP plant $P_{el,nom}$ and the modulation Z, which is defined as

$$Z = \frac{P_f}{P_{f,nom}}, \tag{7}$$

with the nominal fuel power $P_{f,nom}$ and Z theoretically ranging between 0 and 1. Within the model, the minimum modulation Z_{min} must be predefined and should always be greater than 0.33 and smaller than 1. P_{el} lies in the range between 50 kW and 18.3 MW according to Berberich et al. (2015). The general empiric relation between Z and the electrical efficiency is defined as:

$$\begin{aligned} \eta_{el} = a_{el} + b_{el} \cdot (Z - Z_{min}) \\ + c_{el} \cdot [\ln(P_{el,nom}) - \ln(P_{el,min})], \end{aligned} \tag{8}$$

where

$$P_{el,min} = P_{el,nom} \cdot Z_{min}, \tag{9}$$

and with the partial derivatives b_{el} and c_{el}. The minimum electrical efficiency a_{el} represents the point from where the tangent plane is spanned. This value can be computed by rearranging the equation and setting in the nominal electrical efficiency $\eta_{el,nom}$ for η_{el} as well as setting Z to 1 (Höfner 2019, p. 16). The parameters b_{el} and c_{el} result out of the research of Berberich et al. (2015) analysing 49 combustion engine CHP plants and are summarized in table 3 (Berberich et al. 2015). In addition to the calculation of the electrical efficiency, the calculation of the thermal efficiency comprises the further variables supply temperature of the heat circuit T_s and the return temperature of the heat circuit T_r. The nominal electrical power $P_{el,nom}$ and the minimum electrical power $P_{el,min}$ need to be replaced in comparison to equation by the corresponding nominal thermal power $P_{th,nom}$ and the minimum thermal power $P_{th,min}$:

$$P_{th,min} = \frac{P_{th,nom}}{P_{el,nom}} \cdot P_{el,min}, \tag{10}$$

which leads to the equation:

$$\begin{aligned} \eta_{th} = a_{th} + b_{th} \cdot (Z - Z_{min}) \\ + c_{th} \cdot [\ln(P_{th,nom}) - \ln(P_{th,min})] \\ + d_{th} \cdot (T_s - T_{s,max}) + e_{th} \cdot (T_r - T_{r,min}) \end{aligned} \tag{11}$$

with the maximum supply $T_{s,max}$ and minimum return temperature $T_{r,min}$. The minimum thermal efficiency equates a_{th} and is reckoned through a rearranging of equation 11. Since the partial derivatives d_{th} and e_{th} have negative signs (compare table 3), a_{th} reaches its minimum if T_s is set to the maximum value and T_r is set to the minimum value. The corresponding terms will be zero. For the calculation of the thermal efficiency η_{th} in equation 11 the modulation Z is needed and redefined as following:

$$Z = \frac{P_{f,\mathrm{tar}}}{P_{f,\mathrm{nom}}} = \frac{P_{th,\mathrm{tar}}}{P_{th,\mathrm{nom}}} \cdot \frac{\eta_{th,\mathrm{nom}}}{\eta_{th}} = X_{th} \cdot \frac{\eta_{th,\mathrm{nom}}}{\eta_{th}}, \tag{12}$$

according to (Berberich et al. 2015, pp. 59–60). Thereby are $P_{f,tar}$ the targeted fuel power and X_{th} the thermal modulation. The equation 11 and equation 12 result in the final equation for η_{th} (Berberich et al. 2015, p. 62):

$$\begin{aligned} \eta_{th} = -\frac{1}{2}\Big\{ & -a_{th} + b_{th} \cdot Z_{min} \\ & - c_{th} \cdot \big[\ln(P_{th,nom}) - \ln(P_{th,min})\big] \\ & - d_{th} \cdot [T_r - T_{r,min}] - e_{th} \cdot [T_s - T_{s,max}] \Big\} \\ & + \Bigg\{ \Bigg(\frac{1}{2}\big(-a_{th} + b_{th} \cdot Z_{min} \\ & - c_{th} \cdot \big[\ln(P_{th,nom}) - \ln(P_{th,min})\big] \\ & - d_{th} \cdot [T_r - T_{r,min}] - e_{th} \cdot [T_s - T_{s,max}] \big) \Bigg)^2 \\ & - b_{th} \cdot X_{th} \cdot \eta_{th,nom} \Bigg\}^{0.5}, \end{aligned} \tag{13}$$

Now the produced electricity P_{el} is determined by:

$$Z = \frac{P_{f,tar}}{P_{f,nom}} = \frac{P_{el}}{P_{el,nom}} \cdot \frac{\eta_{el,nom}}{\eta_{el}}. \tag{14}$$

2.2 Electrolyser

PEMEC are usually selected by the required hydrogen mass flow rates. Mass flow rates from the reaction can be calculated using the following equation with i indicating either water, oxygen or hydrogen:

$$\dot{m}_i = v_i \cdot M_i \cdot \eta_f \cdot N_{cells} \cdot \frac{I_{\mathrm{cell}}}{n \cdot F}, \tag{15}$$

where v_i and M_i are the stoichiometric coefficients and the molar mass, respectively (Sood et al. 2020). These are multiplied by the cell current I_{cell} and divided by the number of moles transferred n and the Faraday constant F

Table 3. Parameters for the calculation of η_{el} and η_{th} according to (Berberich et al. 2015, p. 57)

Parameter	Value	Unit
b_{el}	0.1089	
c_{el}	0.0255	
b_{th}	-0.0746	
c_{th}	-0.0255	
d_{th}	-0.0020	
e_{th}	-0.0017	
Z_{min}	0.33	
Z_{max}	1	
$T_{r,min}$	45	°C
$T_{s,max}$	90	°C

$[9.6485 \cdot 10^4$ C/mol$]$. In this case $n = 2$ and $v_i = 1$ (Sood et al. 2020). η_f represents the Faraday efficiency and N_{cells} the total number of cells within the PEMEC. For calculating I_{cell} losses must be considered. These losses can be expressed by calculating the operating voltage (E) of the PEMEC:

$$E = V_{oc} + V_{act} + V_{ohm} + V_{con}, \tag{16}$$

where V_{oc} represents the open circuit voltage, V_{act} activation voltage, V_{ohm} ohmic voltage and V_{con} the transport voltage. However, V_{con} is negligibly small and do not play a role in this consideration and are therefore not taken into account (Sood et al. 2020). V_{oc} is derived from the Nernst voltage valid for the equilibrium state:

$$V_{oc} = E_0 + \frac{RT}{nF} \cdot \ln\left(\frac{p_{H_2} \cdot \sqrt{p_{O_2}}}{a_{H_2O}}\right), \tag{17}$$

with

$$E_0 = \frac{\Delta G}{nF} = 1.229 \text{ V}, \tag{18}$$

where R stands for the universal gas constant $[8.31447$ J/(mol K)$]$, p_i for the partial pressures of the respective substances involved and T for the temperature in Kelvin. The partial pressures of hydrogen and oxygen are typically determined by the system design. The water activity a_{H_2O} between electrode and membrane corresponds to 1, because water is fed to the cell (Ruiz Diaz 2021). The reversible cell voltage E_0 is then calculated with the Gibbs free energy ΔG $[237.22$ kJ/mol$]$ at standard conditions (Abdin et al. 2015; Ruiz Diaz 2021).

For calculating V_{ohm} the resistance R_{ohm} is needed which mainly includes the resistance due to the membrane and other resistances of the cell components R_{other}:

$$R_{ohm} = \frac{d_{mem}}{\sigma_{mem}} + R_{other}. \tag{19}$$

The quantity d_{mem} denotes the thickness of the membrane. The reference value of $180\,\mu$m was used according to Ojong (2018). R_{other} must be determined experimentally (Sood et al. 2020). The proton conductivity σ_{mem} of the membrane is directly related to the membrane hydration and the operating temperature. For PEM fuel cells, the proton conductivity of the Nafion®- membrane has been studied in detail and can be empirically expressed as a function of membrane hydration and temperature:

$$\sigma_{mem} = (0.005139\lambda - 0.00326) \cdot e^{\left[1268\left(303^{-1} - T^{-1}\right)\right]}, \tag{20}$$

where λ is the hydration number of the membrane, which varies from 14 to 25 (Ojong 2018; Ruiz Diaz 2021; Sood et al. 2020). The degree of hydration of the membrane plays a crucial role in the performance of low-temperature PEM fuel cells. It shows considerable variation, which makes it a critical parameter for determining fuel cell efficiency. On the other hand, for PEM water electrolysis cells, where water is the main transport medium, it is usually assumed that the membrane is always fully hydrated. This is why the hydration number is estimated to be ($\lambda \approx 24$) (Ojong 2018). V_{ohm} can be determined with the use of the cell current I_{cell} or with the cell current density J_{cell} as following:

$$V_{ohm} = \frac{I_{cell}}{R_{ohm}} = \frac{d_{mem}}{\sigma_{mem}} J_{cell}. \tag{21}$$

For the calculation of V_{act}, the exchange current density needs to be obtained. This is typically done with the Butler–Volmer equation:

$$J_{cell} = J_{0,k}\left[e^{\left(\frac{\alpha_k nF}{RT} V_{act,k}\right)} - e^{\left(-\frac{(1-\alpha_k)nF}{RT} V_{act,k}\right)}\right], \tag{22}$$

where α_k is the symmetry factor, $J_{0,k}$ is the current exchange density at k which represents either anode or cathode (Ojong 2018; Ruiz Diaz 2021; Sood et al. 2020). Furthermore J_{cell} can be determined by using the area content of the membrane A_{mem} according to Sood et al. (2020):

$$J_{cell} = \frac{I_{cell}}{A_{mem}}. \tag{23}$$

Lastly the activation voltage $V_{act,k}$ at the anode or cathode can be expressed by the following equation:

$$V_{act,k} = \frac{RT}{F} \sinh^{-1}\left(\frac{J_{\text{cell}}}{2J_{0,k}}\right). \tag{24}$$

$J_{0,k}$ must be determined for cathode and anode using a reference exchange current density J_0^{ref}:

$$J_{0,k} = J_0^{\text{ref}} e^{\left(-\frac{E_{act,k}}{RT}\right)}, \tag{25}$$

where the activation energy $E_{act,k}$ for cathode and anode must be determined experimentally (Ojong 2018; Sood et al. 2020). However, there are publications that use a simplified model using only the exchange current density $J_{0,k}$ without a reference value. **Table 4** gives an overview of

the research results from which the values of Abdin et al. (2015) seem to fit best to this PEMEC model. Other tables can be found in the literature or have to be determined experimentally (Carmo et al. 2013; Ojong 2018; Sood et al. 2020).

Table 4. Overview of electrokinetic parameters. Abdin et al. (2015) parameters were applied.

Parameter	**Abdin et al. (2015)**	Liso et al. (2018)	Marangio et al. (2009)	Ni et al. (2006)
$J_{0,\text{anode}}$	10^{-3}	$5 \cdot 10^{-9}$	10^{-2}	10^{-2}
$J_{0,\text{cathode}}$	10^{3}	10	10	10^{5}
α_{anode}	0.8	1.2	2	0.5
α_{cathode}	0.25	0.5	0.5	0.5

The three important efficiencies to consider are the Faraday efficiency η_f, cell efficiency η_{cell} and the energy efficiency η_e. The Faraday efficiency represents the correlation between the actual and presumed efficiency of the produced hydrogen output and is expressed as:

$$\eta_f = \frac{\dot{m} \cdot n \cdot F}{I \cdot M_{H_2}}. \tag{26}$$

The voltage efficiency η_v is the ratio of the thermoneutral voltage V_{tn}, also called the minimum required voltage, and the actual cell voltage V_{cell}. This requires the work enthalpy ΔH [237.22 kJ/mol] at standard conditions and is expressed as:

$$V_{tn} = \frac{\Delta H}{nF} = 1.48\,\text{V}, \tag{27}$$

$$\eta_v = \frac{V_{tn}}{V_{cell}}. \tag{28}$$

Here the losses due to pressure, mass transport and activation are taken into account (Ruiz Diaz 2021). At this point it is possible to determine the overall efficiency of the cell:

$$\eta_{cell} = \eta_f \cdot \eta_v. \tag{29}$$

Additionally, the energy efficiency is calculated as the ratio of the benefit, measured as H_2 mass flow expressed in generated watts, to the input, the energy balance:

$$\eta_e = \frac{\dot{m} \cdot HHV}{P_{el} - \dot{Q}_{he} + \dot{Q}_{add}}. \tag{30}$$

where HHV is the higher heating value of hydrogen (39.4 kWh/kg) (Bender et al. 2020, p. 805). In addition to the electrical power P_{el}, the heat recovered from the heat exchangers $\dot{Q}_{he}$ and the heat supplied to the system $\dot{Q}_{add}$ may be included in the energy balance.

2.3 Hydrogen storage and compressor

The hydrogen storage dynamics are governed by the equation:

$$p_i = p_0 + CF \cdot \frac{\dot{m}_{H_2} \cdot R \cdot T}{V_{bottle} \cdot n_{bottle} \cdot M_{H_2}}, \tag{31}$$

where p_i is the pressure inside the storage tank, p_0 the initial pressure, CF the correction factor, $\dot{m}_{H_2}$ the mass flow rate of hydrogen, V_{bottle} and n_{bottle} denote the bottle's volume and number of bottles, respectively (Albarghot et al. 2019; Gorgun 2006; Onar et al. 2006). The system is designed with a maximum pressure p_{max} of 80 bar, an initial pressure p_0 of 1 bar, and a bottle volume V_{bottle} of 50 litres, mirroring laboratory setups, and n_{bottle} indicates the count of such bottles. The correction factor (CF), integral to the equation, adjusts for deviations from ideal gas behaviour, essentially a temperature and pressure-dependent ratio of real to ideal gas volumes (Zucker et al. 2019, p. 327). It is equal to one at pressures below 138 bar at ambient temperature, reflecting the model's assumption of a constant room temperature and a slow storage process with a maximum pressure of 80 bar, thus simplifying CF to one for this scenario (McCarty et al. 1981). Using this information the state of charge (SOC) of the storage can be calculated:

$$SOC = \frac{p_i}{p_{max}}. \tag{32}$$

An isothermal compressor has been implemented, assuming an ideal gas as the compression pressures are low. The power of the ideal compressor P_{com} is defined as an integral over the volume flow rate:

$$P_{com} = -\int (p - p_u)\, d\dot{V}, \tag{33}$$

where p is the compression pressure and p_u is the ambient pressure. Using the efficiency η_{com}, the effective compression power required P_{req} can be calculated in terms of electrical power needed:

$$P_{el,req} = \frac{P_{com}}{\eta_{com}}. \tag{34}$$

2.4 Control Strategies

The control strategies play a crucial role in the performance of the energy system. First, a BAT management control sequence has been implemented based on Lu et al. (2019), as the Modelica Buildings library does not offer one. The CHP unit within the heating system plays the most important role. This is because very small or very large heat loads can not be met by the CHP unit, either because it is uneconomical or because the size of the engine does not allow it. The whole control sequence is shown in **Figure 1**, where TES is the thermal energy storage, HP is the heat pump and U is the user. The control system always checks if the TES is charged. If not, the minimum threshold is checked and if this is exceeded, the CHP is switched on. It is switched off when the heat load is no longer required or when the TES is fully charged.

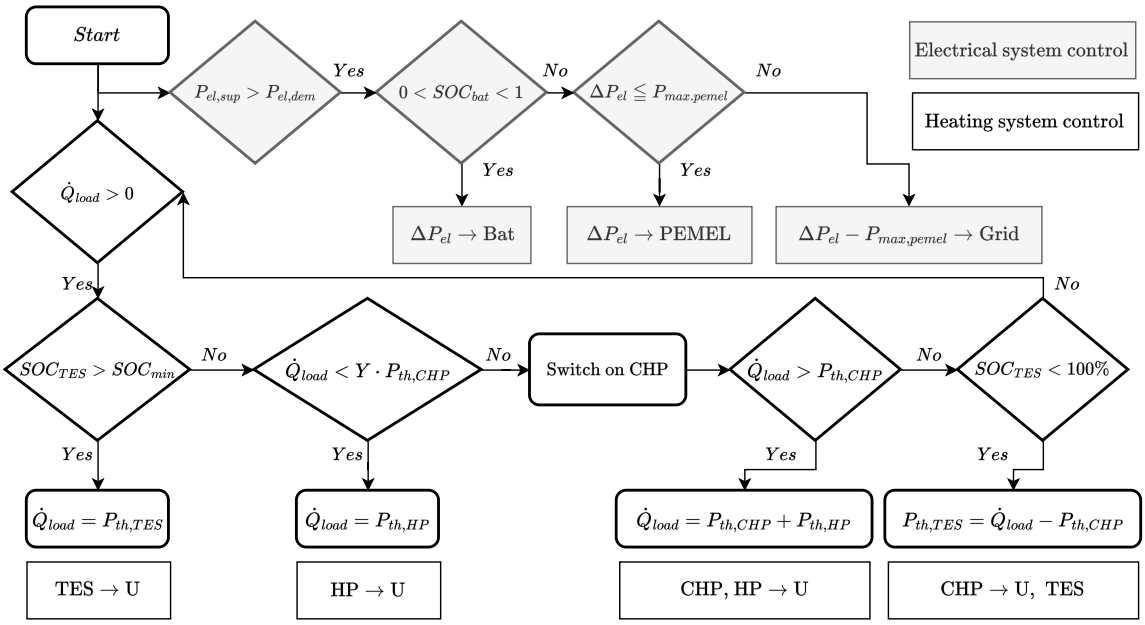

Figure 1. Control sequence of the implemented heating and electrical system

In general, it is possible to operate industrial PEMECs in a grid-connected manner. However, in applications for buildings with smaller PEMECs, low electricity prices are very important to ensure economic viability. For this reason, only self-produced electricity by e.g. PV is used for operation. In case a BAT has been implemented as well, excess energy should first be stored in the BAT before using it for hydrogen production, in order to reduce losses due to lower PEMEC efficiencies. This control sequence is also shown in Figure 1, where ΔP_{el} is the difference between the supplied electrical power $P_{el,sup}$ and the demand $P_{el,dem}$. The power requirement of the compressor is always included when the PEMEC is in operation. If the supply exceeds the PEMEC capacity and the BAT is fully charged, the excess energy is sold to the grid.

Additionally the CHP only runs when sufficient hydrogen is in the tank and is turned off when the hydrogen tank is empty. Similarly to the PEMEC as shown in **Figure 2**.

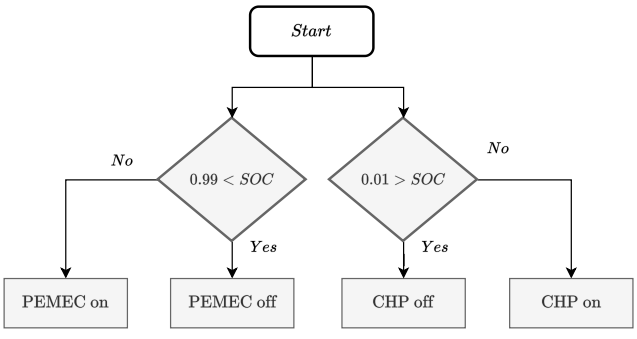

Figure 2. Control sequences of the hydrogen tank.

2.5 CO_2e Calculation

For calculating CO_2e emissions the emission factors need to be known. Sources of CO_2e emissions include combustion of methane gas (202 gCO_2e/kWh (Umweltbundesamt 2023a)) and electricity production, varying by location and energy mix. In 2022, emission factors were 366 gCO_2e/kWh for Germany and 66 gCO_2e/kWh for France (European Environment Agency 2023). Using only green electricity, emission factors differ based on the renewable source, ranging from 4 gCO_2e/kWh for hydro power to 475 gCO_2e/kWh for liquid biomass (Lauf et al. 2022, p. 40). The estimated green emission factors are approximately 66 gCO_2e/kWh for Germany and 31 gCO_2e/kWh for France, reflecting their respective green energy mixes (Arbeitsgruppe Erneuerbare Energien-Statistik 2024; L'Agence ORE et al. 2024).

3 Validation

Laboratory measurements, literature, and manufacturer data were utilized to validate the PEMEC and gas engine CHP models. Technical data are provided in the appendix in **Table 8** and **Table 9**. Initially, the PEMEC's validation involved conducting measurements at different hydrogen outlet pressures (6, 8, and 10 bar) in the university laboratory. **Table 5** is a summary of the measured values compared with the simulation results at a 6 bar outlet pressure, with the relative deviation, ν, calculated using the theoretical value as a reference. This procedure was also applied to data measured at 8 and 10 bar, revealing an average relative deviation of 10%.

Due to its high complexity the modulation model needed to be validated. Höfner (2019) has developed a model specifically for CHP, rather than a general ap-

proach. Their efficiency curves are therefore suitable for comparison and validation, as also shown in **Figure 3**. Furthermore, the university has the manufacturer's specifications for a hydrogen-fuelled CHP unit, which are compared with the simulation results in **Figure 4**. A deviation is present, yet it remains within acceptable limits. Note that both gas engine CHP units are from the same manufacturer (compare **Table 8**) (2G Energy AG 2024).

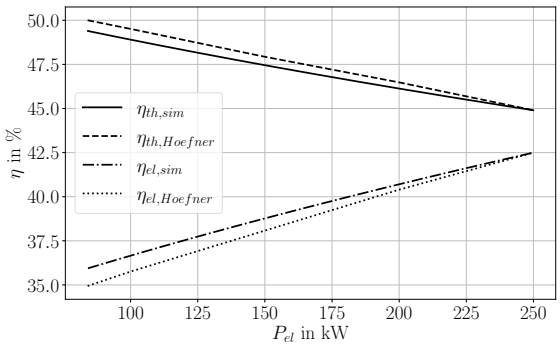

Figure 3. Comparison of Simulation Efficiencies and Höfner (2019) Efficiencies of agenitor 406 Gas Engine CHP

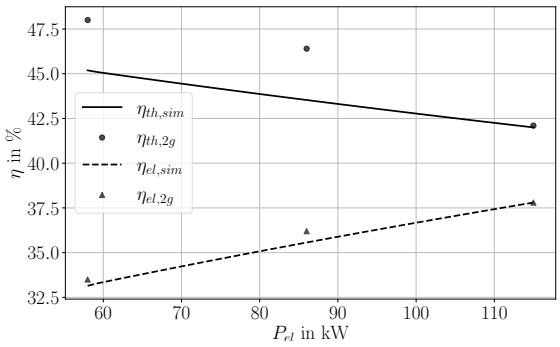

Figure 4. Comparison of Simulation Efficiencies and Manufacturer Specification of agenitor 404 H_2 Gas Engine CHP

Table 5. Comparison of measurements and simulation at 6 bar outlet pressure and $\dot{V}$ in Nm^3/h

P_{el}	$\dot{V}_{H_2,real}$	$\dot{V}_{H_2,sim}$	ν
334.5	0.050	0.054	0.08
555.0	0.100	0.090	0.11
817.7	0.150	0.133	0.13
1138.8	0.200	0.185	0.08
1357.8	0.222	0.220	0.01

4 Case Study

For this project, the city of Offenburg provided hourly data for heat and electricity consumption, used in all simulations. In agreement with project partners, the five buildings were treated as one system to achieve climate neutrality, requiring the system to be designed around the CHP, which needs to be dimensioned first. The CHP aims to cover the base heat demands while the HP operates as supportive heat generator.Here, the classic mode of operation of a gas-fuelled CHP unit is copied for hydrogen-fuelled units .

The dimensioning of a heat-guided CHP plant relies on the descending sorted annual load duration curve of the consumer. The economic optimum for the classical CHP and a peak load boiler, an HP, is sought, aiming for 5,000 to 6,000 full utilization hours or 10% to 30% coverage of thermal heat demand (Arbeitsgruppe Erneuerbare Energien-Statistik 2015; Sokratherm GmbH n.d.; Verbraucherzentrale 20.05.2021). 4,000 full utilisation hours or 15% of nominal thermal capacity at maximum heating demand was chosen as these buildings have no domestic hot water demand and low summer heating demand. The optimal fit would be a CHP with a nominal thermal capacity range $P_{th,nom}$ of 33 to 38 kW. A commercially available hydrogen CHP was chosen, the smallest available being the MAH 33.3 TI 311A from MAMOTEC energy solutions (see technical data in **Table 6**) (MAMotec GmbH 2024).

Table 6. Technical data of hydrogen and natural gas CHP (MAMotec GmbH 2024).

	MAH 33.3 TI 311A
Fuel	Hydrogen
P_{el}	38 kW
P_{th}	53.7 kW
η_{el}	35.5 %
η_{th}	50.2 %
η_{total}	85.7 %

Given that Offenburg will not be connected to the European hydrogen grid until at least 2030, a decentralized, standalone operation is more realistic in the near future. Hydrogen is produced by PEMEC, stored in tanks, and then burned by a CHP when needed. Most of the electricity demand is met by renewable energy sources, with excess energy stored in a BAT and used to operate the PEMEC.

The low density of hydrogen poses storage challenges, with the hydrogen tank being the limiting factor. Large tanks can serve as seasonal hydrogen sinks but require significant space and investment. Therefore, the hydrogen tank size will be investigated through a sweep, keeping the PV size constant. The tank pressure is maintained at 80 bar throughout the study.

Before investigating different tank sizes, the PEMEC size must be determined. Several test simulations indicated that a 500 kW PEMEC is optimal due to the uniformity of hydrogen production, resulting in high full load hours for the PEMEC. Diversifying the electricity mix

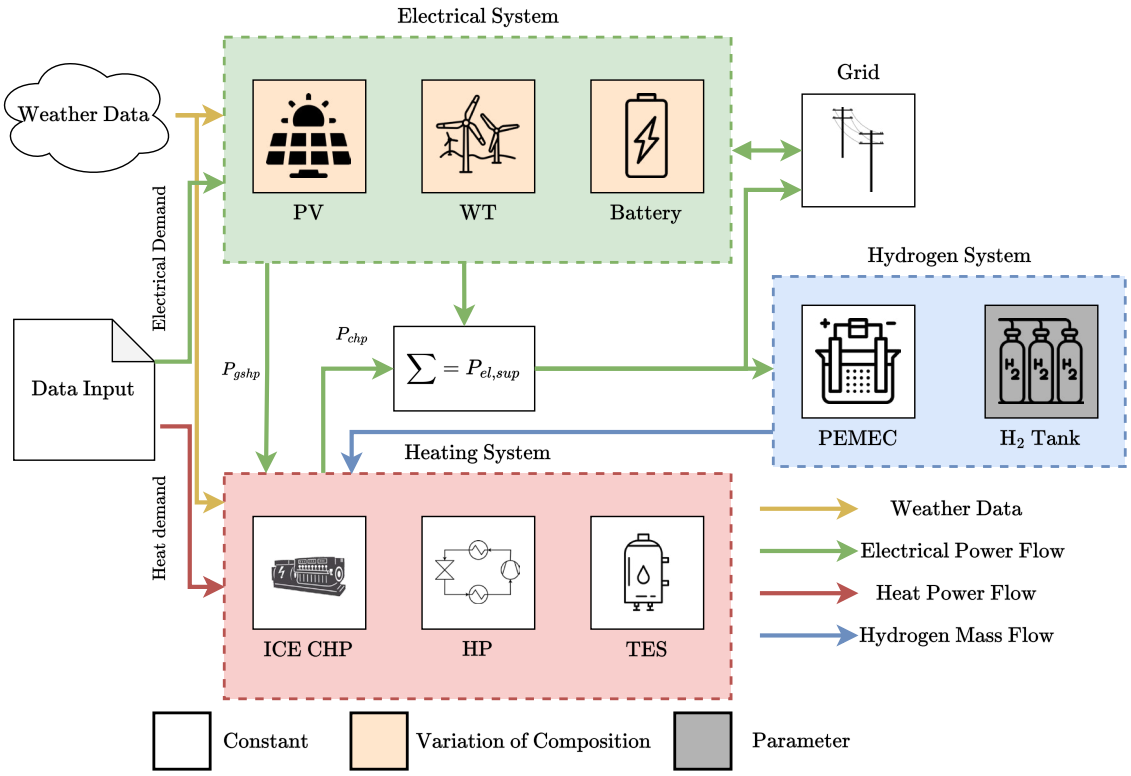

Figure 5. Schematic set up of the decentralised stand-alone operation scenario with a modulation CHP

with PV and Wind Turbines (WT) is prudent. Reducing the PV area to provide the required amount of renewable energy is cost-efficient, while reducing the size of a WT is more challenging form a technical point of view.

Figure 5 shows the schematic structure of this scenario. The Modelica model was implemented identically to the schematic setup. The orange blocks indicate the variation combination, the grey block indicates the parameter for the sweep, and the white blocks indicate constants throughout the sweeps. Only the modulation operation strategy of the CHP is investigated, based on previous results. These showed that with this described control strategy and under the condition that hydrogen can be supplied at any time, the modulation CHP needed 900 kg less hydrogen per year than a stationary CHP (13,700 kg). The downside is a worse efficiency and less heat coverage of only 56% compared to 59%. As the production of hydrogen is very expensive, it should only be used sparingly. For this reason, the modulation was chosen.

5 Results

A total of six scenarios are considered and CO_2e emissions are calculated for comparison as this is the target to be reduced. The results are summarised in **Figure 6**. The labels indicate the composition of the scenario according to **Table 7**.

Figure 6 shows the emissions in tonnes of CO_2e for different storage capacities. Sources of emissions during operation are from natural gas combustion or depending on the electricity demand emission factor (see section 2.5). Since only hydrogen is burned, all emissions are due to the electricity required from the grid. In this scenario, only green electricity was consumed, using the estimated green emission factor of 66 gCO_2e/kWh for Germany. It demonstrates that the combination of PV, WT, and BAT leads to the lowest emissions. Nevertheless, due to drought periods where no electricity is produced, this strategy is unable to entirely eliminate emissions. It also states that the WT generated by this facility is insufficient for its intended purpose. Consequently, it would be necessary to expand the plant. However, the geographical location is not optimal for the generation of wind power.

Furthermore an increase in the size of the hydrogen storage tank has a negligible impact on emissions from a volume of 500 m^3, particularly when WT and PV are com-

Table 7. Dimensioning and composition of the decentralised energy system with the MAH 33.3 TI 311A CHP.

Description	PV	PV and WT
CHP	38 kW_{el}, 53.7 kW_{th}	38 kW_{el}, 53.7 kW_{th}
PV	1.8 MWp	0.9 MWp
BAT	500 kWh	500 kWh
WT	-	0.5 MWp
HP	197 kW	197 kW

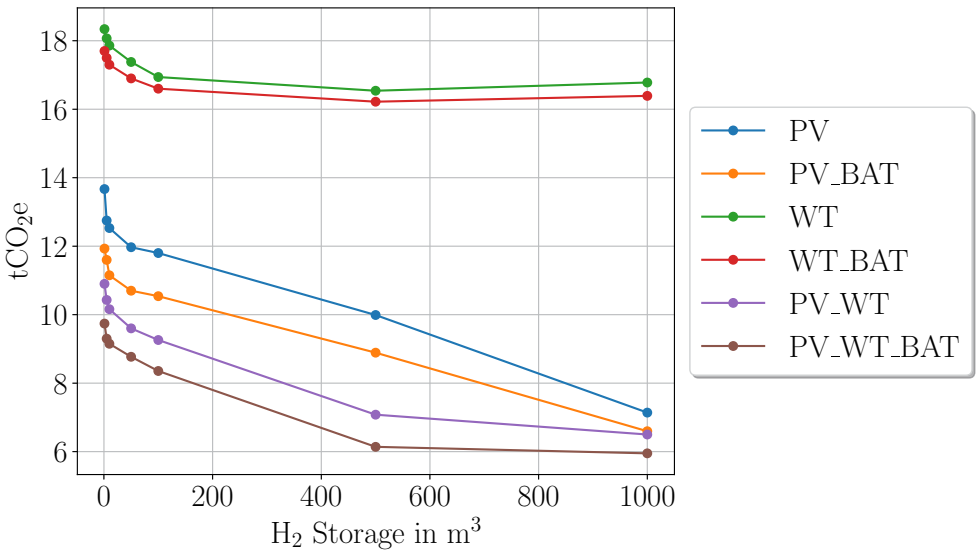

Figure 6. CO_2e emissions depending on hydrogen storage size (at 80 bar)

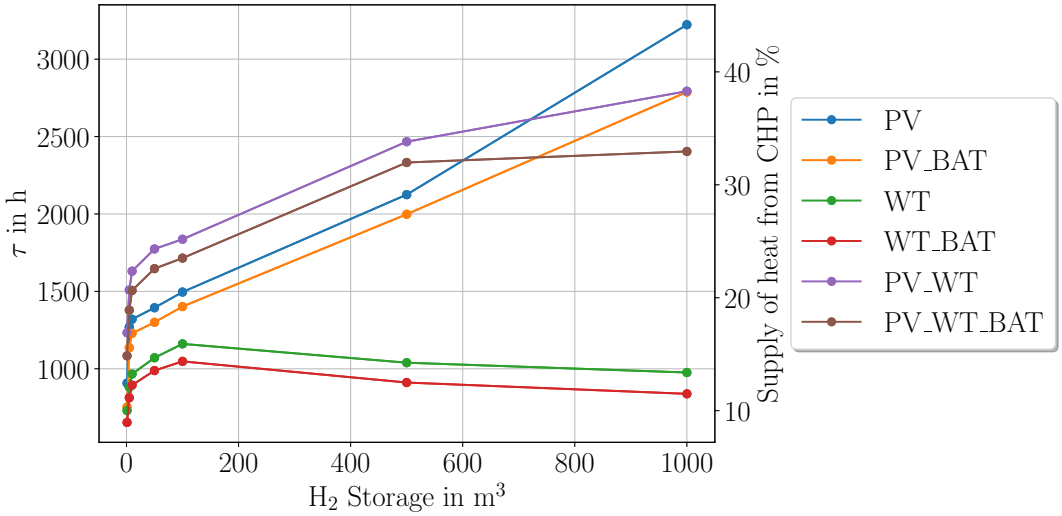

Figure 7. Full utilisation hours and heat coverage of the CHP.

bined. However, tank sizes larger than 50 m^3 are unrealistically large. Therefore, the feasibility of such a system needs to be investigated using other control strategies.

The full utilization hours of the CHP depend on hydrogen production. This depends on the amount of electrical energy available, the size of the PEMEC, and the size of the hydrogen tank. For this reason, the **Figure 7** shows that the full utilization hours also increase as the tank size increases. The only exceptions are the two scenarios where wind power is the sole source of electricity. In these cases, the full load hours decrease as the tank size increases due to the minimum threshold of the control system, which means the tank can only be emptied when a certain amount is available. Here, the electricity production of the WT is clearly too low. Conversely, the highest full utilization hours can be achieved with pure PV and a larger hydrogen storage tank.

6 Discussion and Outlook

In this paper, the feasibility of a hydrogen-powered gas engine CHP unit in a decentralised energy system has been investigated using a real use case with data from the city of Offenburg in Germany. The ultimate goal is to reduce emissions in order to achieve carbon neutrality or come close to this target.

The results of the simulation models indicate several

promising benefits of hydrogen CHP units. In particular, this system can significantly reduce carbon emissions when integrated into decentralised energy systems. However, hydrogen storage requires a lot of space, which is questionable in real-world conditions and probably not realistic. Smaller storage sizes already reduce CO_2e, but other operating strategies may be more efficient in terms of CO_2e emissions and need to be compared while considering costs as well. Therefore, a new control strategy needs to be investigated, where the CHP covering only peak heat demand.

A cost calculation has already been added, calculating investment and operating costs, as well as the levelized costs of electricity and hydrogen. In the future, the calculation of CO_2 emissions will be improved by including emissions from the manufacture of the equipment used. In addition, improvements to the empirical approach are being considered with the CHP units available in the laboratory, as well as improvements to all other models using measured data from the university laboratory where possible. For example, by implementing a hydrogen tank with higher storage pressures. For a continuation of this project, an optimisation tool could be used to optimally dimension the system.

Please refer to the link for the latest version of the model: `https://github.com/IKKUengine/CO2InnO-H2-CHP-Demonstrator`.

Acknowledgements

This work was co-funded by Interreg through the CO2InnO project. The authors would like to thank Lukas Stahl and René Behmann for their early support in implementing the software. Special thanks to Natalie Miller and Yamit Ibarrasuarez from the City of Offenburg for their cooperation.

References

2G Energy AG (2024). *agenitor | 75-450 kW | Der globale Effizienzmaßstab : 2G Energy*. URL: https://2-g.com/de/produkte/agenitor (visited on 2024-02-15).

Abdin, Z., CJ. Webb, and E.MacA. Gray (2015). "Modelling and simulation of a proton exchange membrane (PEM) electrolyser cell". In: *International Journal of Hydrogen Energy* 40.39, pp. 13243–13257. ISSN: 0360-3199. DOI: 10.1016/j.ijhydene.2015.07.129.

Albarghot, Mohamed M. et al. (2019). "Sizing and Dynamic Modeling of a Power System for the MUN Explorer Autonomous Underwater Vehicle Using a Fuel Cell and Batteries". In: *Journal of Energy* 2019, pp. 1–17. ISSN: 2356-735X. DOI: 10.1155/2019/4531497.

Arbeitsgruppe Erneuerbare Energien-Statistik (2015). *BHKW-Fibel: Wissen in kompakter Form*. Essen: energieDRUCK Verlag für sparsamen und umweltfreundlichen Energieverbrauch. URL: https://asue.de/sites/default/files/asue/themen/blockheizkraftwerke/2015/broschueren/asue_050315_bhkw_fibel.pdf.

Arbeitsgruppe Erneuerbare Energien-Statistik (2024-03-08). *Erneuerbare Energien in Zahlen*. Umweltbundesamt. Publisher: Umweltbundesamt. URL: www.umweltbundesamt.de/themen/klima-energie/erneuerbare-energien/erneuerbare-energien-in-zahlen#uberblick (visited on 2024-04-23).

Bender, Beate and Göhlich Dietmar, eds. (2020). *Dubbel Taschenbuch für den Maschinenbau 1: Grundlagen und Tabellen*. 26th ed. Vol. 1. Berlin: Springer. ISBN: 978-3-662-59710-1. DOI: 10.1007/978-3-662-59711-8.

Berberich, Magdalena et al. (2015). *SOLAR-KWK – Entwicklung multifunktionaler Systeme zur solar unterstützten Kraft-Wärme-Kopplung – solare Fernwärme und saisonale Wärmespeicher für die Energiewende*. Stuttgart.

Carmo, Marcelo et al. (2013). "A comprehensive review on PEM water electrolysis". In: *International Journal of Hydrogen Energy* 38.12, pp. 4901–4934. ISSN: 0360-3199. DOI: 10.1016/j.ijhydene.2013.01.151.

Danish Energy Agency (2024). *Technology Catalogues*. The Danish Energy Agency. URL: www.ens.dk/en/our-services/technology-catalogues (visited on 2024-04-10).

Ellamla, Harikishan R. et al. (2015-10-20). "Current status of fuel cell based combined heat and power systems for residential sector". In: *Journal of Power Sources* 293, pp. 312–328. ISSN: 0378-7753. DOI: 10.1016/j.jpowsour.2015.05.050.

Elmer, Theo et al. (2015-02). "Fuel cell technology for domestic built environment applications: State of-the-art review". In: *Renewable and Sustainable Energy Reviews* 42, pp. 913–931. ISSN: 13640321. DOI: 10.1016/j.rser.2014.10.080.

European Environment Agency (2023). *Greenhouse gas emission intensity of electricity generation*. Greenhouse gas emission intensity of electricity generation. URL: www.eea.europa.eu/data-and-maps/daviz/co2-emission-intensity-14/#tab-googlechartid_chart_41 (visited on 2024-04-23).

European Hydrogen Backbone (2024). *The European Hydrogen Backbone (EHB) initiative | EHB European Hydrogen Backbone*. URL: www.ehb.eu (visited on 2024-01-04).

Gorgun, H. (2006). "Dynamic modelling of a proton exchange membrane (PEM) electrolyzer". In: *International Journal of Hydrogen Energy* 31.1, pp. 29–38. ISSN: 03603199. DOI: 10.1016/j.ijhydene.2005.04.001.

Höfner, Peter (2019). *Vergleich strom- und wärmegeführter Betriebsweise eines BHKW im Nahwärmenetz mit Langzeitwärmespeicher*. Vienna.

L'Agence ORE et al. (2024-03-08). *Panorama de l'électricité renouvelable*. URL: www.assets.rte-france.com/prod/public/2023-07/2023-07-19-panorama-energies-renouvelables-2022.pdf (visited on 2022-12-31).

Lauf, Thomas, Michael Memmler, and Sven Schneider (2022-12-09). *Emissionsbilanz erneuerbarer Energieträger 2021*. Umweltbundesamt. 170 pp. URL: www.umweltbundesamt.de/publikationen/emissionsbilanz-erneuerbarer-energietraeger-2021 (visited on 2024-04-23).

Liso, Vincenzo et al. (2018). "Modelling and Experimental Analysis of a Polymer Electrolyte Membrane Water Electrolysis Cell at Different Operating Temperatures". In: *Energies* 11.12. ISSN: 1996-1073. DOI: 10.3390/en11123273.

Lu, Xing et al. (2019). "An Open Source Modeling Framework for Interdependent Energy-Transportation-Communication Infrastructure in Smart and Connected Communities". In: *IEEE Access* 7. Conference Name: IEEE Access, pp. 55458–55476. ISSN: 2169-3536. DOI: 10.1109/ACCESS.2019.2913630.

MAMotec GmbH (2024). *Gasmotoren Überciht*. URL: https://mamotec-online.de/gasmotoren-uebersicht/ (visited on 2024-06-03).

Marangio, F., M. Santarelli, and M. Calì (2009). "Theoretical model and experimental analysis of a high pressure PEM water electrolyser for hydrogen production". In: *International Journal of Hydrogen Energy* 34.3, pp. 1143–1158. ISSN: 0360-3199. DOI: 10.1016/j.ijhydene.2008.11.083.

McCarty, RD., J. Hord, and H. M. Roder (1981). *Selected properties of hydrogen (engineering design data)*. URL: https://nvlpubs.nist.gov/nistpubs/Legacy/MONO/nbsmonograph168.pdf.

Ni, Meng, Mkh Leung, and Y. C. Leung (2006). "Electrochemistry Modeling of Proton Exchange Membrane (PEM) Water Electrolysis for Hydrogen Production". In: *Semantic Scholar*. URL: https://api.semanticscholar.org/CorpusID:45236790.

Ojong, Tabu Emile (2018). *Characterization of the Performance of PEM Water Electrolysis Cells operating with and without Flow Channels, based on Experimentally Validated Semi-empirical Coupled-Physics Models*. Ed. by Fraunhofer. DOI: 10.24406/publica-fhg-282794.

Onar, O. C., M. Uzunoglu, and M. S. Alam (2006). "Dynamic modeling, design and simulation of a wind/fuel cell/ultra-capacitor-based hybrid power generation system". In: *Journal of Power Sources* 161.1, pp. 707–722. ISSN: 03787753. DOI: 10.1016/j.jpowsour.2006.03.055.

Reuters (2023-11-14). "Wasserstoff: Robert Habeck kündigt fast 10.000 Kilometer langes Netz an". In: *Der Spiegel*. ISSN: 2195-1349. URL: www.spiegel.de/wirtschaft/unternehmen/habeck-kuendigt-fast-10-000-kilometer-langes-wasserstoffnetz-an-a-2821473f-6e07-47dd-a1f0-15c9ab45f6a6 (visited on 2023-11-22).

Ruhnau, Oliver, Lion Hirth, and Aaron Praktiknjo (2019-10-01). "Time series of heat demand and heat pump efficiency for energy system modeling". In: *Scientific Data* 6.1. Publisher: Nature Publishing Group, p. 189. ISSN: 2052-4463. DOI: 10.1038/s41597-019-0199-y.

Ruiz Diaz, Daniela Fernanda (2021). *Mathematical Modeling of Polymer Electrolyte Membrane Water Electrolysis Cell with a Component-level Approach*. Ed. by UC Irvine. URL: https://escholarship.org/uc/item/8cv660cn.

Sokratherm GmbH (n.d.). *Dimensioning of CHP units up to 2 MWel*. URL: https://www.sokratherm.de/wp-content/uploads/auslegungsgrundsaetze-08-1-wm-eng.pdf.

Sood, Sumit et al. (2020). "Generic Dynamical Model of PEM Electrolyser under Intermittent Sources". In: *Energies* 13.24. ISSN: 1996-1073. DOI: 10.3390/en13246556.

Umweltbundesamt (2023a-10-31). *Kohlendioxid-Emissionsfaktoren für die deutsche Berichterstattung atmosphärischer Emissionen*. URL: https://view.officeapps.live.com/op/view.aspx?src=https%3A%2F%2Fwww.umweltbundesamt.de%2Fsites%2Fdefault%2Ffiles%2Fmedien%2F361%2Fdokumente%2Fco2_ef_liste_2024_brennstoffe_und_industrie_final.xlsx&wdOrigin=BROWSELINK (visited on 2024-05-08).

Umweltbundesamt (2023b-05-02). *Treibhausgasminderungsziele Deutschlands*. Umweltbundesamt. Publisher: Umweltbundesamt. URL: www.umweltbundesamt.de/daten/klima/treibhausgasminderungsziele-deutschlands (visited on 2023-11-08).

Verbraucherzentrale (20.05.2021). *Kleine Blockheizkraftwerke: Die Heizung, die auch Strom liefert*. URL: https://www.verbraucherzentrale.de/wissen/energie/heizen-und-warmwasser/kleine-blockheizkraftwerke-die-heizung-die-auch-strom-liefert-6007.

Wetter, Michael et al. (2014). "Modelica Buildings library". In: *Journal of Building Performance Simulation* 7.4, pp. 253–270. DOI: https://doi.org/10.1080/19401493.2013.765506.

Zucker, Robert D. and Oscar Biblarz (2019). *Fundamentals of gas dynamics*. 3rd ed. Hoboken, NJ: Wiley. ISBN: 978-1-119-48170-6.

Appendix

Table 8. Technical data of the gas engine CHP units (2G Energy AG 2024; Höfner 2019)

	agenitor 404c H_2	agenitor 404	agenitor 406
P_{el}	115 *kW*	100 *kW*	250 *kW*
P_{th}	129 *kW*	130 *kW*	264 *kW*
η_{el}	0.377	0.384	0.425
η_{th}	0.423	0.499	0.449
η_{total}	0.80	0.883	0.874

Table 9. Technical data PEMEC

	Value	Unit
n_{cell}	10	-
n_{stack}	1	-
$P_{\text{el,max}}$	1900	W
p	0 - 10	bar
V_{op}	230	V
$\dot{V}_{H_2,\text{max}}$	0.3	Nm^3/h